Astronomy & Astrophysics manuscript no. aa
December 7, 2025

Predicting NBA Team Performance: From Historical Standings to Player-level Forecasts

Weihao Li[1,⋆], Shuhao Gao[1], C. Brassac[1], and C. Estievenart[1]

McCormick School of Engineering, Northwestern University
e-mail: {weihaoli2027, shuhaogao2027, author3, author4}@u.northwestern.edu

Received December 8, 2025

ABSTRACT

Context. Optional, leave empty if necessary. The heading "Context" is used when needed to give background information on the research conducted in the paper
Aims. Mandatory. The objectives of the paper are defined here.
Methods. Mandatory. The methods of the investigation are outlined here
Results. Mandatory. The results are summarized here.
Conclusions. Optional, leave empty if necessary. "Conclusions" can be used to explicit the general conclusions that can be drawn from the paper.

Key words. giant planet formation – κ-mechanism – stability of gas spheres

1. Introduction

In this project, we study how well different approaches can predict NBA team performance. Our goal is straightforward: given past data, can we forecast how many games each team will win in a future season? To explore this question, we compare two models that rely on fundamentally different sources of information.

The first model is a simple team-level baseline that uses only historical standings. For any pair of seasons within the past twenty years, we examine how a team's previous win total relates to its win total in another season. This provides a direct, standings-based method for predicting future performance without considering player-level factors.

The second model takes a player-centered perspective. We collect long-term statistics for both retired and still-active NBA players and train a model to learn how player performance tends to evolve over time. Using these learned patterns, we predict next-season box-score statistics for current active players and then aggregate the projected player output to estimate each team's future win total.

By comparing these two approaches, we aim to understand when a simple standings-based baseline is sufficient and when a more detailed, player-based forecasting pipeline provides an advantage, particularly in seasons affected by significant roster changes.

2. Prior Literature

2.1. Team-level rating and expectation models

A large body of work in sports analytics has focused on predicting team performance using aggregate team-level statistics. One influential family of models is the *Pythagorean expectation*, which estimates a team's theoretical winning percentage from points scored and points allowed via a power-law relationship. Originally proposed for baseball and later adapted to basketball, this idea underlies many simple baselines that relate scoring margins to wins and losses (see, e.g., **??**). These models provide strong, easy-to-interpret benchmarks but depend solely on aggregate scoring margins and do not incorporate information about individual players.

Another common approach is to model team strength with rating systems inspired by Elo. In basketball applications, Elo-style ratings are updated after each game based on the result, home-court advantage, and the margin of victory, and then used to forecast future game and series outcomes. Public-facing systems such as FiveThirtyEight's NBA model illustrate how dynamic ratings can track changes in team strength over a season and provide reasonably accurate probabilistic predictions for both games and playoff series (**?**). Together, Pythagorean and Elo-style systems represent static or quasi-static team-level baselines that are closely related to our first model, which relies on historical team wins and standings. However, because these methods operate on aggregate team outcomes, they are inherently limited in their ability to anticipate abrupt changes in performance driven by roster turnover or player development.

2.2. Machine learning for NBA game and season prediction

Beyond analytic formulas and rating systems, many studies have applied machine learning to predict basketball results using team-level features. Early work by **?** used neural networks to predict single-game NBA outcomes from box-score statistics and contextual variables, demonstrating that nonlinear models can capture interactions between basic team statistics. More recent surveys review a wide range of approaches, including logistic regression, support vector machines, tree-based ensembles, and deep neural networks, and typically find that machine-learning

⋆ Corresponding author: wli@u.northwestern.edu

models outperform simpler statistical baselines when sufficient historical data are available (**?**).

Researchers have also moved from game-level prediction to season-level tasks, such as forecasting a team's final win total or playoff qualification. For example, **?** regress regular-season wins on team-level and aggregated player statistics to study which factors are most predictive of team success. These season-level models again treat each team as the unit of analysis and usually rely on summary statistics from the current or previous season.

2.3. Player-level prediction and its link to team performance

Complementary to team-level approaches, a growing literature studies player evaluation and performance prediction using detailed box-score and tracking data. **?** review many of these methods, including regression-based models for player efficiency metrics, clustering techniques for grouping players with similar playing styles, and rating systems that quantify individual contribution to team success. In practice, coaches and analysts often combine such player-level models with domain knowledge to support decisions about rotations, matchups, and roster construction.

Some work, including **?**, aggregates player statistics into team-level features to predict season outcomes, effectively creating a simple player-to-team pipeline. However, existing player-focused models typically train and evaluate on overlapping time periods for the same set of players, and they rarely combine long-run player evolution with explicit team-level baselines.

In contrast, our project is designed to learn generic player evolution patterns from a historical cohort that includes both retired and still-active players, and then apply these patterns to predict the next-season performance of currently active players. We subsequently aggregate predicted player statistics to the team level and compare the resulting win forecasts to those from a simple standings-based baseline over roughly two decades of NBA data. This setup allows us to evaluate how a player-based forecasting pipeline and a standings-based model perform side by side, especially in seasons where teams undergo substantial roster changes.

3. Citations and maths examples

In this section the one-zone model of **?**, originally used to study the Cepheïd pulsation mechanism, will be briefly reviewed, see Fig. **??**, Table **??** and Eq. (**??**). For the one-zone-model Baker obtains necessary conditions for dynamical, secular and vibrational (or pulsational) stability (Eqs. (34a, b, c) in Baker **?**).

$$\tau_{\rm co} = \frac{E_{\rm th}}{L_{r0}}\,, \tag{1}$$

and the *local free-fall time*

$$\tau_{\rm ff} = \sqrt{\frac{3\pi}{32G}\frac{4\pi r_0^3}{3M_{\rm r}}}\,, \tag{2}$$

Baker's K and σ_0 have the following form:

$$\sigma_0 = \frac{\pi}{\sqrt{8}}\frac{1}{\tau_{\rm ff}} \tag{3}$$

$$K = \frac{\sqrt{32}}{\pi}\frac{1}{\delta}\frac{\tau_{\rm ff}}{\tau_{\rm co}}\,; \tag{4}$$

where $E_{\rm th} \approx m(P_0/\rho_0)$ has been used and

$$\begin{aligned}\delta &= -\left(\tfrac{\partial \ln \rho}{\partial \ln T}\right)_P \\ e &= mc^2\end{aligned} \tag{5}$$

is a thermodynamical quantity which is of order 1 and equal to 1 for nonreacting mixtures of classical perfect gases. The physical meaning of σ_0 and K is clearly visible in the equations above. σ_0 represents a frequency of the order one per free-fall time. K is proportional to the ratio of the free-fall time and the cooling time. Substituting into Baker's criteria, using thermodynamic identities and definitions of thermodynamic quantities,

$$\Gamma_1 = \left(\frac{\partial \ln P}{\partial \ln \rho}\right)_S\,,\ \chi_\rho = \left(\frac{\partial \ln P}{\partial \ln \rho}\right)_T\,,\ \kappa_P = \left(\frac{\partial \ln \kappa}{\partial \ln P}\right)_T$$

$$\nabla_{\rm ad} = \left(\frac{\partial \ln T}{\partial \ln P}\right)_S\,,\ \chi_T = \left(\frac{\partial \ln P}{\partial \ln T}\right)_\rho\,,\ \kappa_T = \left(\frac{\partial \ln \kappa}{\partial \ln T}\right)_T$$

4. Figures examples

Examples of figures using graphicx. The guide "Using Imported Graphics in LaTeX2e" by Keith Reckdahl is available on a lot of LaTeXpublic servers or CTAN mirrors.

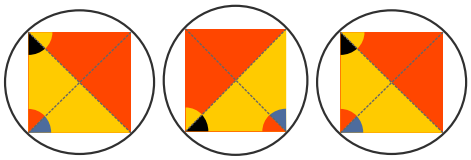

Fig. 1: A onecolumn \figure* with six graphics

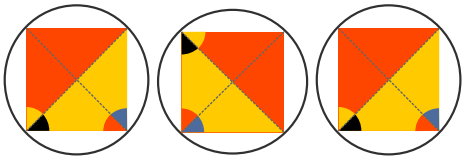

Fig. 1: continued.

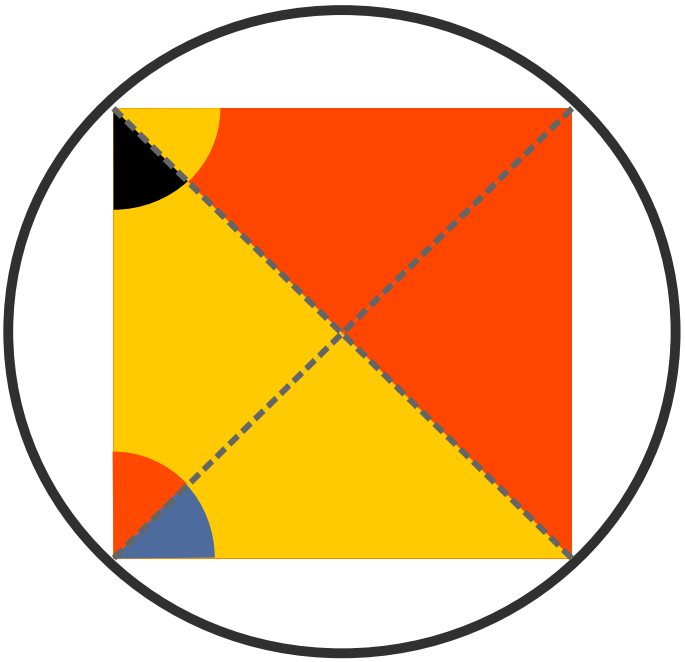

Fig. 2: Figure as large as the column width

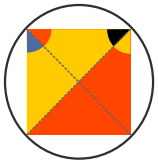

Fig. 3: Rotated figure

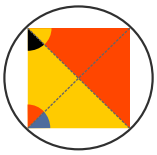

Fig. 4. Figure with caption on the right side

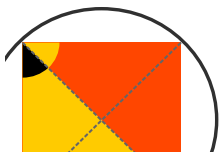

Fig. 5: Figure with a new BoundingBox

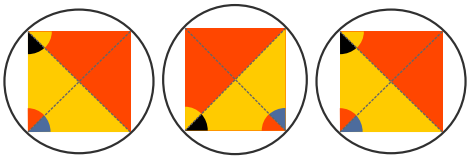

Fig. 6: A figure including three graphics

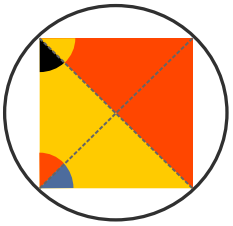

Fig. 7: Continued figure numbering

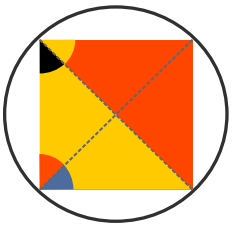

Fig. 7: continued.

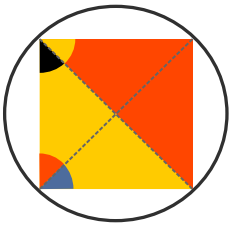

Fig. 7: continued.

5. Tables examples

The jump in table numbering below is caused by the command \longtable*. This command only works in the onecolumn environment. For this reason, we recommend either:

- placing your long tables in onecolumn appendices (cf. **??** and **??**),
- or using the longtab environment as illustrated by tables **??** and **??**. Note that the longtab environment will preserve the table numbering and automatically places long tables after the appendices. They will be moved inside the appendices by the Publisher, if necessary.

Table 1: Simple A&A Table

HJD	E	Method#2	Method#3
1	50	−837	970
2	47	877	230

Table 4: Table with notes

Star	Spectral type	RA(J2000)
69	B1 V	09 15 54.046
LS 1267 (86)	O8 V	09 15 52.787
24.6	7.58	1.37
MO 2-119	B0.5 V	09 15 33.7
LS 1269	O8.5 V	09 15 56.60

Notes. The top panel shows likely members of Pismis 11. The bottom panel displays stars outside the clusters.

Table 5: Table with multiple notes

Star	Spectral type	RA(J2000)
69	B1 V	09 15 54.046
LS 1267 (86)	O8 V	11.07[a]
24.6	7.58[l]	1.37[a]
MO 2-119	B0.5 V	11.74[c]
LS 1269	O8.5 V	10.85[d]

Notes. The top panel shows likely members of Pismis 11. The bottom panel displays stars outside the clusters.
[(a)] Photometry for MF13, LS 1267 and HD 80077 from Dupont et al. [(b)] Photometry for LS 1262, LS 1269 from Durand et al. [(c)] Photometry for MO2-119 from Mathieu et al.

Table 6: Table with references

SN name	Epoch (with respect to B maximum)	Bands
1981B	0	*UBV*
1990N	2, 7	*UBVRI*
1991M	3	*VRI*
	SNe 91bg-like	
1991bg	1, 2	*BVRI*
1999by	−5, −4, −3, 3, 4, 5	*UBVRI*
	SNe 91T-like	
1991T	−3, 0	*UBVRI*
2000cx	−3, −2, 0, 1, 5	*UBVRI*

References. (1) **?**; (2) **?**; (3) **?**; (4) **?**; (5) **?**; (6) **?**; (7) **?**; (8) **?**.

6. Conclusions

Lorem ipsum dolor sit amet, consectetuer adipiscing elit. In hac habitasse platea dictumst. In- teger tempus convallis augue. Etiam facilisis.

Acknowledgements. Part of this work was supported by *ESO*, project number Ts 17/2–1.

References

FiveThirtyEight. 2015, How Our NBA Predictions Work, https://fivethirtyeight.com/features/how-our-nba-predictions-work/, accessed: 2025-12-07
Loeffelholz, B., Bednar, E., & Bauer, M. 2009, Journal of Quantitative Analysis in Sports, 5
Oliver, D. 2004, Basketball on Paper: Rules and Tools for Performance Analysis (Washington, DC: Potomac Books)
Sarlis, P. & Tjortjis, C. 2020, Information Systems, 93, 101562
Yang, J. 2015, Predicting Regular Season Results of NBA Teams Based on Regression Analysis of Common Basketball Statistics, UC Berkeley Statistics Project

Appendix A: Wide tables and figures after an appendix title: recommended method

In the PDF output, floats should be placed under their own appendix, not before the title, nor after the title of the next appendix. In short appendices, one-column floats {figure*} or {table*} will generate a blank page. To prevent this behaviour, we recommend to switch to \onecolumn and set the [ht!] parameter in your floats: please check the LaTeXcode of this appendix.

In case you have a lot of floating objects for little text and the LaTeXengine moves the floats away from their context, the command \FloatBarrier of the "placeins" package will empty the float buffer and place all stored floats in the continuity. If you still encounter problems with wide floats placement, just use the \onecolumn environment throughout the appendices.

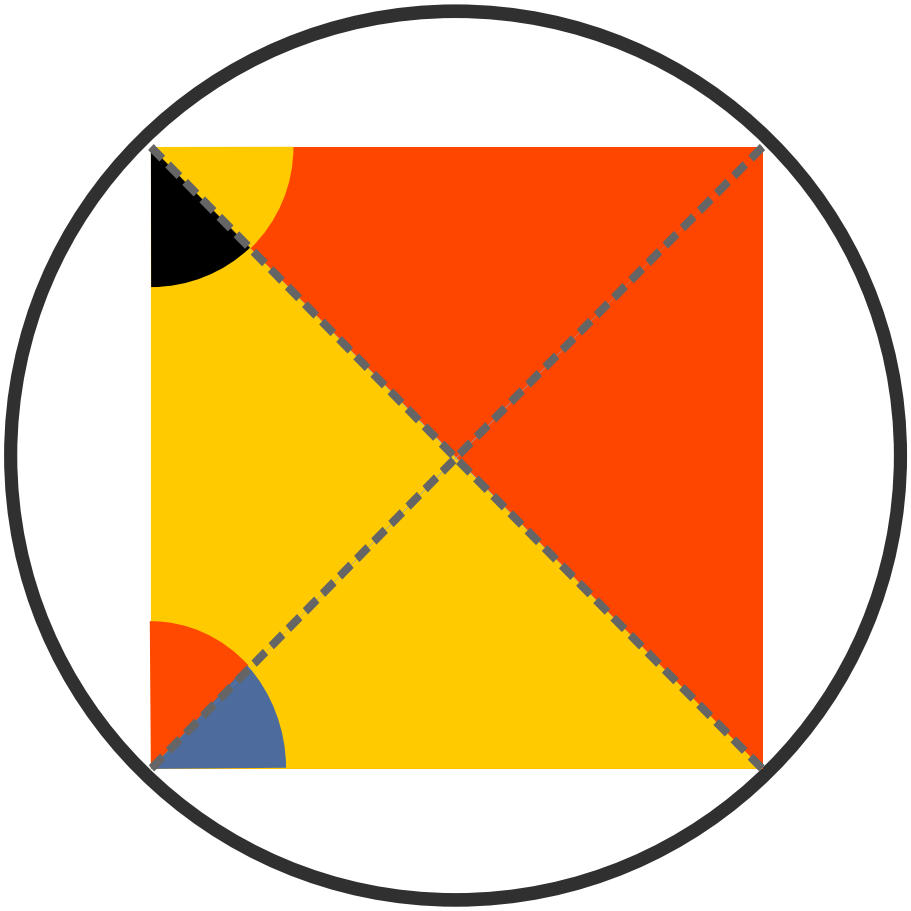

Fig. A.1: A one-column {figure*}[ht!] after a section title. If text follows like below, it is easier to finish the section in \onecolumn. If needed, you may revert to \twocolumn when reaching the next page.

Lorem ipsum dolor sit amet, consectetuer adipiscing elit. Ut purus elit, vestibulum ut, placerat ac, adipiscing vitae, felis. Curabitur dictum gravida mauris. Nam arcu libero, nonummy eget, consectetuer id, vulputate a, magna. Donec vehicula augue eu neque. Pellentesque habitant morbi tristique senectus et netus et malesuada fames ac turpis egestas. Mauris ut leo. Cras viverra metus rhoncus sem. Nulla et lectus vestibulum urna fringilla ultrices. Phasellus eu tellus sit amet tortor gravida placerat. Integer sapien est, iaculis in, pretium quis, viverra ac, nunc. Praesent eget sem vel leo ultrices bibendum. Aenean faucibus. Morbi dolor nulla, malesuada eu, pulvinar at, mollis ac, nulla. Curabitur auctor semper nulla. Donec varius orci eget risus. Duis nibh mi, congue eu, accumsan eleifend, sagittis quis, diam. Duis eget orci sit amet orci dignissim rutrum.

Nam dui ligula, fringilla a, euismod sodales, sollicitudin vel, wisi. Morbi auctor lorem non justo. Nam lacus libero, pretium at, lobortis vitae, ultricies et, tellus. Donec aliquet, tortor sed accumsan bibendum, erat ligula aliquet magna, vitae ornare odio metus a mi. Morbi ac orci et nisl hendrerit mollis. Suspendisse ut massa. Cras nec ante. Pellentesque a nulla. Cum sociis natoque penatibus et magnis dis parturient montes, nascetur ridiculus mus. Aliquam tincidunt urna. Nulla ullamcorper vestibulum turpis. Pellentesque cursus luctus mauris.

Appendix B: Wide tables and figures after an appendix title: alternate method

To prevent a blank page, a second method is to insert the appendix title after declaring the onecolumn float.
This method should be reserved to appendices containing only one-column floats{figure*} or {table*} and no text.

Table B.1: A one-column {table*}

ISO-L1551	$F_{6.7}$ [mJy]	$\alpha_{6.7-14.3}$	YSO type[d]	Status	Comments
			New YSO candidates		
1	1.56 ± 0.47	–	Class II[c]	New	Mid
2	0.79:	0.97:	Class II ?	New	
3	4.95 ± 0.68	3.18	Class II / III	New	
5	1.44 ± 0.33	1.88	Class II	New	
1	1.56 ± 0.47	–	Class II[c]	New	Mid
2	0.79:	0.97:	Class II ?	New	
3	4.95 ± 0.68	3.18	Class II / III	New	
5	1.44 ± 0.33	1.88	Class II	New	
1	1.56 ± 0.47	–	Class II[c]	New	Mid
2	0.79:	0.97:	Class II ?	New	
3	4.95 ± 0.68	3.18	Class II / III	New	
5	1.44 ± 0.33	1.88	Class II	New	
1	1.56 ± 0.47	–	Class II[c]	New	Mid
2	0.79:	0.97:	Class II ?	New	
3	4.95 ± 0.68	3.18	Class II / III	New	
5	1.44 ± 0.33	1.88	Class II	New	
2	0.79:	0.97:	Class II ?	New	
3	4.95 ± 0.68	3.18	Class II / III	New	
5	1.44 ± 0.33	1.88	Class II	New	
1	1.56 ± 0.47	–	Class II[c]	New	Mid
2	0.79:	0.97:	Class II ?	New	
3	4.95 ± 0.68	3.18	Class II / III	New	
5	1.44 ± 0.33	1.88	Class II	New	
1	1.56 ± 0.47	–	Class II[c]	New	Mid
2	0.79:	0.97:	Class II ?	New	
3	4.95 ± 0.68	3.18	Class II / III	New	
5	1.44 ± 0.33	1.88	Class II	New	
1	1.56 ± 0.47	–	Class II[c]	New	Mid
2	0.79:	0.97:	Class II ?	New	
3	4.95 ± 0.68	3.18	Class II / III	New	
5	1.44 ± 0.33	1.88	Class II	New	
			Previously known YSOs		
61	0.89 ± 0.58	1.77	Class I	HH 30	Circumstellar disk
96	38.34 ± 0.71	37.5	Class II	MHO 5	Spectral type

Appendix C: Long tables in appendices

For long tables (multipage) in appendices, we use the method described in appendix A. For long landscape tables, please refer to Appendix E.

Appendix D: Rotated single page tables

To prevent a blank page with {sidewaystable*}, we use the method described in appendix B: declare the table first, and the section second.

Table D.1: A rotated table with {sidewaystable*}

ISO-L1551	$F_{6.7}$ [mJy]	$\alpha_{6.7-14.3}$	YSO type[d]	Status	Comments
New YSO candidates					
1	1.56 ± 0.47	–	Class II[c]	New	Mid
2	0.79:	0.97:	Class II ?	New	
3	4.95 ± 0.68	3.18	Class II / III	New	
5	1.44 ± 0.33	1.88	Class II	New	
1	1.56 ± 0.47	–	Class II[c]	New	Mid
2	0.79:	0.97:	Class II ?	New	
3	4.95 ± 0.68	3.18	Class II / III	New	
5	1.44 ± 0.33	1.88	Class II	New	
1	1.56 ± 0.47	–	Class II[c]	New	Mid
2	0.79:	0.97:	Class II ?	New	
3	4.95 ± 0.68	3.18	Class II / III	New	
5	1.44 ± 0.33	1.88	Class II	New	
1	1.56 ± 0.47	–	Class II[c]	New	Mid
2	0.79:	0.97:	Class II ?	New	
3	4.95 ± 0.68	3.18	Class II / III	New	
5	1.44 ± 0.33	1.88	Class II	New	
1	1.56 ± 0.47	–	Class II[c]	New	Mid
2	0.79:	0.97:	Class II ?	New	
3	4.95 ± 0.68	3.18	Class II / III	New	
5	1.44 ± 0.33	1.88	Class II	New	
1	1.56 ± 0.47	–	Class II[c]	New	Mid
2	0.79:	0.97:	Class II ?	New	
3	4.95 ± 0.68	3.18	Class II / III	New	
5	1.44 ± 0.33	1.88	Class II	New	
1	1.56 ± 0.47	–	Class II[c]	New	Mid
2	0.79:	0.97:	Class II ?	New	
3	4.95 ± 0.68	3.18	Class II / III	New	
5	1.44 ± 0.33	1.88	Class II	New	
Previously known YSOs					
61	0.89 ± 0.58	1.77	Class I	HH 30	Circumstellar disk
96	38.34 ± 0.71	37.5	Class II	MHO 5	Spectral type

Appendix E: Rotated long tables in appendices

For rotated long tables in appendices, we use the method described in appendix A, combined with {landscape}.

Table E.1: A long landscape table

Catalogue	M_V	Spectral	Distance	Mode	Count Rate
Gl 33	6.37	K2 V	7.46	S	0.043170
Gl 66AB	6.26	K2 V	8.15	S	0.260478
Gl 68	5.87	K1 V	7.47	P	0.026610
				H	0.008686
Gl 86 [1]	5.92	K0 V	10.91	S	0.058230
Gl 33	6.37	K2 V	7.46	S	0.043170
Gl 66AB	6.26	K2 V	8.15	S	0.260478
Gl 68	5.87	K1 V	7.47	P	0.026610
				H	0.008686
Gl 86	5.92	K0 V	10.91	S	0.058230
Gl 33	6.37	K2 V	7.46	S	0.043170
Gl 66AB	6.26	K2 V	8.15	S	0.260478
Gl 68	5.87	K1 V	7.47	P	0.026610
				H	0.008686
Gl 86	5.92	K0 V	10.91	S	0.058230
Gl 33	6.37	K2 V	7.46	S	0.043170
Gl 66AB	6.26	K2 V	8.15	S	0.260478
Gl 68	5.87	K1 V	7.47	P	0.026610
				H	0.008686
Gl 86	5.92	K0 V	10.91	S	0.058230
Gl 33	6.37	K2 V	7.46	S	0.043170
Gl 66AB	6.26	K2 V	8.15	S	0.260478
Gl 68	5.87	K1 V	7.47	P	0.026610
				H	0.008686
Gl 86	5.92	K0 V	10.91	S	0.058230
Gl 33	6.37	K2 V	7.46	S	0.043170
Gl 66AB	6.26	K2 V	8.15	S	0.260478
Gl 68	5.87	K1 V	7.47	P	0.026610
				H	0.008686
Gl 86	5.92	K0 V	10.91	S	0.058230
Gl 33	6.37	K2 V	7.46	S	0.043170
Gl 66AB	6.26	K2 V	8.15	S	0.260478
Gl 68	5.87	K1 V	7.47	P	0.026610
				H	0.008686
Gl 86	5.92	K0 V	10.91	S	0.058230
Gl 33	6.37	K2 V	7.46	S	0.043170
Gl 66AB	6.26	K2 V	8.15	S	0.260478
Gl 68	5.87	K1 V	7.47	P	0.026610
				H	0.008686

[1] Source not included in the HRI catalog. See Sect. 5.4.2 for details.

Table E.1: continued.

Catalogue	M_V	Spectral	Distance	Mode	Count Rate
Gl 86	5.92	K0 V	10.91	S	0.058230
Gl 33	6.37	K2 V	7.46	S	0.043170
Gl 66AB	6.26	K2 V	8.15	S	0.260478
Gl 68	5.87	K1 V	7.47	P	0.026610
				H	0.008686
Gl 86	5.92	K0 V	10.91	S	0.058230
Gl 33	6.37	K2 V	7.46	S	0.043170
Gl 66AB	6.26	K2 V	8.15	S	0.260478
Gl 68	5.87	K1 V	7.47	P	0.026610
				H	0.008686
Gl 86	5.92	K0 V	10.91	S	0.058230
Gl 33	6.37	K2 V	7.46	S	0.043170
Gl 66AB	6.26	K2 V	8.15	S	0.260478
Gl 68	5.87	K1 V	7.47	P	0.026610
				H	0.008686
Gl 86	5.92	K0 V	10.91	S	0.058230
Gl 33	6.37	K2 V	7.46	S	0.043170
Gl 66AB	6.26	K2 V	8.15	S	0.260478
Gl 68	5.87	K1 V	7.47	P	0.026610
				H	0.008686
Gl 86	5.92	K0 V	10.91	S	0.058230
Gl 33	6.37	K2 V	7.46	S	0.043170
Gl 66AB	6.26	K2 V	8.15	S	0.260478
Gl 68	5.87	K1 V	7.47	P	0.026610
				H	0.008686
Gl 86	5.92	K0 V	10.91	S	0.058230
Gl 33	6.37	K2 V	7.46	S	0.043170
Gl 66AB	6.26	K2 V	8.15	S	0.260478
Gl 68	5.87	K1 V	7.47	P	0.026610
				H	0.008686
Gl 86	5.92	K0 V	10.91	S	0.058230

Table 2: A long table using the longtab environment

Catalogue	M_V	Spectral	Distance	Mode	Count Rate
Gl 33	6.37	K2 V	7.46	S	0.043170
Gl 66AB	6.26	K2 V	8.15	S	0.260478
Gl 68	5.87	K1 V	7.47	P	0.026610
				H	0.008686
Gl 86 [2]	5.92	K0 V	10.91	S	0.058230
	5.92	K0 V	10.91	S	0.058230
Gl 33	6.37	K2 V	7.46	S	0.043170
Gl 66AB	6.26	K2 V	8.15	S	0.260478
Gl 68	5.87	K1 V	7.47	P	0.026610
				H	0.008686
Gl 86	5.92	K0 V	10.91	S	0.058230
Gl 33	6.37	K2 V	7.46	S	0.043170
Gl 66AB	6.26	K2 V	8.15	S	0.260478
Gl 68	5.87	K1 V	7.47	P	0.026610
				H	0.008686
Gl 86	5.92	K0 V	10.91	S	0.058230
Gl 33	6.37	K2 V	7.46	S	0.043170
Gl 66AB	6.26	K2 V	8.15	S	0.260478
Gl 68	5.87	K1 V	7.47	P	0.026610
				H	0.008686
Gl 86	5.92	K0 V	10.91	S	0.058230
Gl 33	6.37	K2 V	7.46	S	0.043170
Gl 66AB	6.26	K2 V	8.15	S	0.260478
Gl 68	5.87	K1 V	7.47	P	0.026610
				H	0.008686
Gl 86	5.92	K0 V	10.91	S	0.058230
Gl 33	6.37	K2 V	7.46	S	0.043170
Gl 66AB	6.26	K2 V	8.15	S	0.260478
Gl 68	5.87	K1 V	7.47	P	0.026610
				H	0.008686
Gl 86	5.92	K0 V	10.91	S	0.058230
	5.92	K0 V	10.91	S	0.058230
Gl 33	6.37	K2 V	7.46	S	0.043170
Gl 66AB	6.26	K2 V	8.15	S	0.260478
Gl 68	5.87	K1 V	7.47	P	0.026610
				H	0.008686
Gl 86	5.92	K0 V	10.91	S	0.058230
	5.92	K0 V	10.91	S	0.058230
Gl 33	6.37	K2 V	7.46	S	0.043170
Gl 66AB	6.26	K2 V	8.15	S	0.260478
Gl 68	5.87	K1 V	7.47	P	0.026610
				H	0.008686
Gl 86	5.92	K0 V	10.91	S	0.058230
	5.92	K0 V	10.91	S	0.058230
Gl 33	6.37	K2 V	7.46	S	0.043170
Gl 66AB	6.26	K2 V	8.15	S	0.260478
Gl 68	5.87	K1 V	7.47	P	0.026610
				H	0.008686
Gl 86	5.92	K0 V	10.91	S	0.058230
	5.92	K0 V	10.91	S	0.058230
Gl 33	6.37	K2 V	7.46	S	0.043170
Gl 66AB	6.26	K2 V	8.15	S	0.260478
Gl 68	5.87	K1 V	7.47	P	0.026610
				H	0.008686
Gl 86	5.92	K0 V	10.91	S	0.058230
	5.92	K0 V	10.91	S	0.058230
Gl 33	6.37	K2 V	7.46	S	0.043170
Gl 66AB	6.26	K2 V	8.15	S	0.260478

[2] Source not included in the HRI catalog. See Sect. 5.4.2 for details.

Table 2: continued.

Catalogue	M_V	Spectral	Distance	Mode	Count Rate
Gl 68	5.87	K1 V	7.47	P	0.026610
				H	0.008686
Gl 86	5.92	K0 V	10.91	S	0.058230
	5.92	K0 V	10.91	S	0.058230
Gl 33	6.37	K2 V	7.46	S	0.043170
Gl 66AB	6.26	K2 V	8.15	S	0.260478
Gl 68	5.87	K1 V	7.47	P	0.026610
				H	0.008686
Gl 86	5.92	K0 V	10.91	S	0.058230
	5.92	K0 V	10.91	S	0.058230
Gl 33	6.37	K2 V	7.46	S	0.043170
Gl 66AB	6.26	K2 V	8.15	S	0.260478
Gl 68	5.87	K1 V	7.47	P	0.026610
				H	0.008686
Gl 86	5.92	K0 V	10.91	S	0.058230
	5.92	K0 V	10.91	S	0.058230
Gl 33	6.37	K2 V	7.46	S	0.043170
Gl 66AB	6.26	K2 V	8.15	S	0.260478
Gl 68	5.87	K1 V	7.47	P	0.026610
				H	0.008686
Gl 86	5.92	K0 V	10.91	S	0.058230
	5.92	K0 V	10.91	S	0.058230
Gl 33	6.37	K2 V	7.46	S	0.043170
Gl 66AB	6.26	K2 V	8.15	S	0.260478
Gl 68	5.87	K1 V	7.47	P	0.026610
				H	0.008686
Gl 86	5.92	K0 V	10.91	S	0.058230
	5.92	K0 V	10.91	S	0.058230
Gl 33	6.37	K2 V	7.46	S	0.043170
Gl 66AB	6.26	K2 V	8.15	S	0.260478
Gl 68	5.87	K1 V	7.47	P	0.026610
				H	0.008686
Gl 86	5.92	K0 V	10.91	S	0.058230

Table 3: A long landscape table using the longtab environment

Catalogue	M_V	Spectral	Distance	Mode	Count Rate
Gl 33	6.37	K2 V	7.46	S	0.043170
Gl 66AB	6.26	K2 V	8.15	S	0.260478
Gl 68	5.87	K1 V	7.47	P	0.026610
				H	0.008686
Gl 86 [3]	5.92	K0 V	10.91	S	0.058230
Gl 33	6.37	K2 V	7.46	S	0.043170
Gl 66AB	6.26	K2 V	8.15	S	0.260478
Gl 68	5.87	K1 V	7.47	P	0.026610
				H	0.008686
Gl 86	5.92	K0 V	10.91	S	0.058230
Gl 33	6.37	K2 V	7.46	S	0.043170
Gl 66AB	6.26	K2 V	8.15	S	0.260478
Gl 68	5.87	K1 V	7.47	P	0.026610
				H	0.008686
Gl 86	5.92	K0 V	10.91	S	0.058230
Gl 33	6.37	K2 V	7.46	S	0.043170
Gl 66AB	6.26	K2 V	8.15	S	0.260478
Gl 68	5.87	K1 V	7.47	P	0.026610
				H	0.008686
Gl 86	5.92	K0 V	10.91	S	0.058230
Gl 33	6.37	K2 V	7.46	S	0.043170
Gl 66AB	6.26	K2 V	8.15	S	0.260478
Gl 68	5.87	K1 V	7.47	P	0.026610
				H	0.008686
Gl 86	5.92	K0 V	10.91	S	0.058230
Gl 33	6.37	K2 V	7.46	S	0.043170
Gl 66AB	6.26	K2 V	8.15	S	0.260478
Gl 68	5.87	K1 V	7.47	P	0.026610
				H	0.008686
Gl 86	5.92	K0 V	10.91	S	0.058230
Gl 33	6.37	K2 V	7.46	S	0.043170
Gl 66AB	6.26	K2 V	8.15	S	0.260478
Gl 68	5.87	K1 V	7.47	P	0.026610
				H	0.008686
Gl 86	5.92	K0 V	10.91	S	0.058230
Gl 33	6.37	K2 V	7.46	S	0.043170
Gl 66AB	6.26	K2 V	8.15	S	0.260478
Gl 68	5.87	K1 V	7.47	P	0.026610
				H	0.008686
Gl 86	5.92	K0 V	10.91	S	0.058230
Gl 33	6.37	K2 V	7.46	S	0.043170

[3] Source not included in the HRI catalog. See Sect. 5.4.2 for details.

Table 3: continued.

Catalogue	M_V	Spectral	Distance	Mode	Count Rate
Gl 66AB	6.26	K2 V	8.15	S	0.260478
Gl 68	5.87	K1 V	7.47	P	0.026610
				H	0.008686
Gl 86	5.92	K0 V	10.91	S	0.058230
Gl 33	6.37	K2 V	7.46	S	0.043170
Gl 66AB	6.26	K2 V	8.15	S	0.260478
Gl 68	5.87	K1 V	7.47	P	0.026610
				H	0.008686
Gl 86	5.92	K0 V	10.91	S	0.058230
Gl 33	6.37	K2 V	7.46	S	0.043170
Gl 66AB	6.26	K2 V	8.15	S	0.260478
Gl 68	5.87	K1 V	7.47	P	0.026610
				H	0.008686
Gl 86	5.92	K0 V	10.91	S	0.058230
Gl 33	6.37	K2 V	7.46	S	0.043170
Gl 66AB	6.26	K2 V	8.15	S	0.260478
Gl 68	5.87	K1 V	7.47	P	0.026610
				H	0.008686
Gl 86	5.92	K0 V	10.91	S	0.058230
Gl 33	6.37	K2 V	7.46	S	0.043170
Gl 66AB	6.26	K2 V	8.15	S	0.260478
Gl 68	5.87	K1 V	7.47	P	0.026610
				H	0.008686
Gl 86	5.92	K0 V	10.91	S	0.058230
Gl 33	6.37	K2 V	7.46	S	0.043170
Gl 66AB	6.26	K2 V	8.15	S	0.260478
Gl 68	5.87	K1 V	7.47	P	0.026610
				H	0.008686
Gl 86	5.92	K0 V	10.91	S	0.058230